

Mini-EUSO: A high resolution detector for the study of terrestrial and cosmic UV emission from the International Space Station

Francesca Capel^{a,b,*}, Alexander Belov^{c,d}, Marco Casolino^{e,f}, Pavel Klimov^c, for the JEM-EUSO Collaboration

^a*Department of Physics, KTH Royal Institute of Technology, SE-106 91 Stockholm, Sweden*

^b*The Oskar Klein Centre for Cosmoparticle Physics, SE-106 91 Stockholm, Sweden*

^c*D.V. Skobeltsyn Institute of Nuclear Physics, M.V. Lomonosov Moscow State University, 1(2), Leninskie Gory, 119991, Russia*

^d*Faculty of Physics, M.V. Lomonosov Moscow State University, 1(2), Leninskie Gory, 119991, Russia*

^e*RIKEN, Hirosawa 2-1, Wako-shi, Saitama 351-01, Japan*

^f*Istituto Nazionale di Fisica Nucleare - Sezione di Roma Tor Vergata, Via Carnevale Emanuele, 00173, Italy*

Abstract

The Mini-EUSO instrument is a UV telescope to be placed inside the International Space Station (ISS), looking down on the Earth from a nadir-facing window in the Russian Zvezda module. Mini-EUSO will map the earth in the UV range (300 - 400 nm) with a spatial resolution of 6.11 km and a temporal resolution of 2.5 μ s, offering the opportunity to study a variety of atmospheric events such as transient luminous events (TLEs) and meteors, as well as searching for strange quark matter and bioluminescence. Furthermore, Mini-EUSO will be used to detect space debris to verify the possibility of using a EUSO-class telescope in combination with a high energy laser for space debris remediation. The high-resolution mapping of the UV emissions from Earth orbit allows Mini-EUSO to serve as a pathfinder for the study of Extreme Energy Cosmic Rays (EECRs) from space by the JEM-EUSO collaboration.

Keywords: EECR, fluorescence detection, UV observation, earth observation, ISS, EUSO

*Corresponding author

Email address: `capel@kth.se` (Francesca Capel)

1. Introduction: The EUSO program

At the far end of the cosmic ray energy spectrum, with energies above 50 EeV, lie the elusive Extreme Energy Cosmic Rays (EECRs). At such energies, the flux is as low as 1 particle/km²/century and the effective area that can be observed by a detector is a key feature. The JEM-EUSO Collaboration aims to detect the UV light produced by EECR-induced extensive air showers (EAS) from the vantage point of low Earth orbit, thereby largely increasing the effective detector volume (Adams et al., 2015a, Olinto et al., 2015). In order to lay the groundwork for such unprecedented observations, the JEM-EUSO collaboration has successfully initiated several pathfinder experiments. Mini-EUSO, along with EUSO-TA (Kawasaki et al., 2015), EUSO-Balloon (Scotti and Osteria, 2016), and EUSO-SPB (Wiencke, 2015), forms the next step towards the observation of EECRs from space. Additionally, UV nightglow measurements with a similar resolution to that of Mini-EUSO are currently being conducted by the TUS experiment on board the Lomonosov satellite (Adams et al., 2015b).

Previous relevant studies include NIGHTGLOW (Barbier et al., 2005) and satellite-borne Tatiana (Garipov et al., 2005) experiments. NIGHTGLOW was a balloon-borne UV telescope flying at an altitude of ~ 30 km for a duration of 8 hours, 4 days after the new moon. The mounted telescope was able to rotate, allowing measurements over a range of angles from nadir to 45° to the zenith. The Tatiana satellite carried a UV detector and operated in a polar orbit at 950 km for a duration of ~ 2 years. The detector was a single photomultiplier tube with a wide field of view ($\sim 15^\circ$) and without spatial resolution. The results from both experiments are consistent, reporting that the UV emission from Earth falls in the range of $3 \times 10^{11} - 10^{12}$ photons \cdot m⁻² s⁻¹ sr⁻¹. The UV radiation measured by satellite missions is highly variable due to the presence of clouds, cities, aurora and other factors in the moving field of view. Both Mini-EUSO and TUS will build on these results with higher resolution measurements, as discussed in section 3.1.

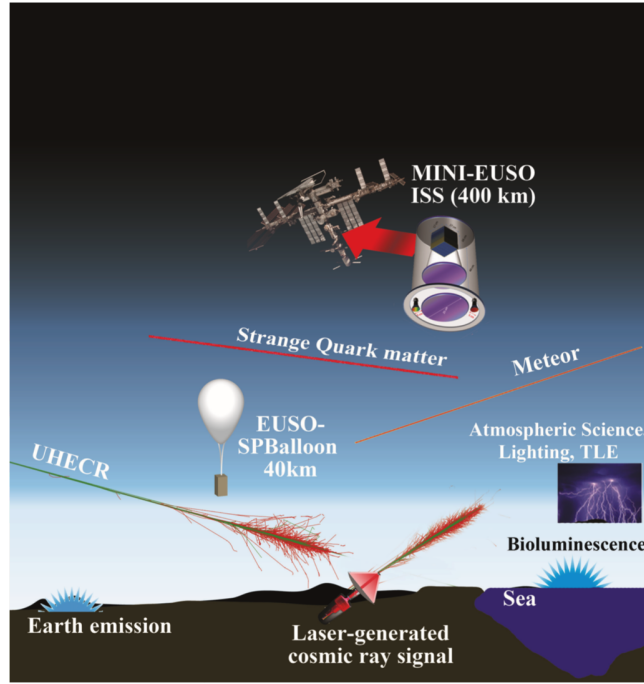


Figure 1: The Mini-EUSO mission summarised in one diagram. From the ISS, Mini-EUSO will observe a variety of interesting phenomena in the UV range, in addition to creating a high resolution UV map of the Earth.

The main goal of Mini-EUSO is to measure the UV emissions from Earth orbit. These observations will provide interesting data for the scientific study of a variety of UV phenomena such as transient luminous events (TLEs), meteors, space debris, strange quark matter (SQM) and bioluminescence, as summarised in Figure 1. Moreover, this will allow the characterisation of the UV emission level, which is essential for the optimisation of the design of future EUSO instruments for EECR detection. Mini-EUSO is approved as a joint project by the Italian (ASI) and Russian (Roscosmos) space agencies and is included in the long-term program of space experiments on the Russian segment of the ISS under the name “UV-Atmosphere”. It is scheduled to be launched to the ISS, where it will be placed at a nadir-facing, UV-transparent window on the Russian Zvezda module. The integration of the instrument is currently at an advanced

stage in order to be compliant with a launch opportunity in late 2017 to early 2018.

2. Instrument overview

Mini-EUSO is based on one EUSO detection unit, referred to as the Photo Detector Module (PDM). The PDM consists of 36 multi-anode photomultiplier tubes (MAPMTs), each with 64 pixels, for a total of 2304 pixels. The MAPMTs are provided by Hamamatsu Photonics, model R11265-M64, and covered with a 2 mm BG3 UV filter with anti-reflective coating. The full Mini-EUSO telescope is made up of 3 main systems, the optical system, the PDM and the data acquisition system. The optical system of 2 Fresnel lenses is used to focus light onto the PDM in order to achieve a large field of view (44°) with a relatively light and compact design, well-suited for space application. The PDM detects UV photons and is read out by the data acquisition system with a sampling rate of $2.5\text{ }\mu\text{s}$ and a spatial resolution of 6.11 km. The key parameters of the instrument are summarised in Table 1.

In addition to the main detector, Mini-EUSO contains two ancillary cameras for complementary measurements in the near infrared (NIR from 1500 to 1600 nm) and visible (VIS from 400 to 780 nm) range. Both cameras are produced by PointGrey. The NIR is a Chameleon 1.3 MP Mono USB 2.0 (CCD: Sony ICX445) coated with phosphorous as an infrared filter, with a resolution of 1296×964 and a maximum frame rate of 18 fps (FLIR Integrated Imaging Solutions, 2017a). The VIS is a Firefly MV 1.3 MP Color USB 2.0 (CMOS: Sony IMX035) with a resolution of 1328×1048 and a maximum frame rate of 23 fps (FLIR Integrated Imaging Solutions, 2017b). A fixed 8.5 mm focal lens provided by Edmund Optics is fitted to each camera. These cameras are placed outside the optical system and acquire data independently of the PDM. The main task of the cameras is to provide atmospheric monitoring in order to better understand the UV luminosity measurements. The complete Mini-EUSO instrument is contained in a box with a connection to ISS for power/grounding

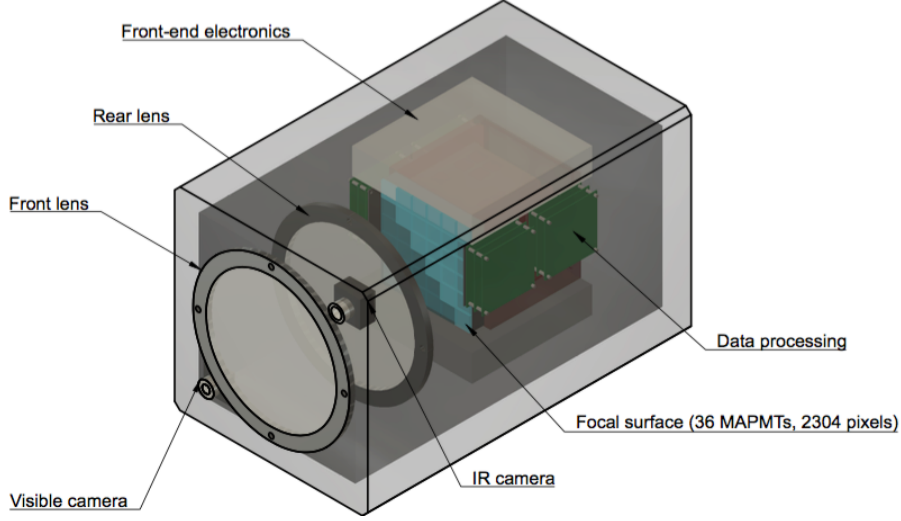


Figure 2: Mini-EUSO conceptual design. The optical system with two double sided Fresnel lenses (25 cm diameter) focuses the UV light on to a focal surface consisting of a single PDM, made up of 36 MAPMTs and 2304 pixels. Ancillary detectors are the visible and near infra-red cameras. The instrument dimensions are $37 \times 37 \times 62 \text{ cm}^3$.

and the interface to the UV-transparent window, from which Mini-EUSO will observe in a fixed position facing the nadir direction. Figure 2 shows the layout of the main systems.

The optical system of Mini-EUSO is composed of two double-sided Fresnel lenses. Each lens is made of PMMA, 25 cm in diameter, 11 mm thick and weighing 0.8 kg. The effective focal length is 300 mm and the field of view is 44° . Ray tracing simulations have been developed to calculate the photon collection efficiency (PCE) of the optical system, defined as the number of photons which arrive in one pixel size divided by the number of photons incident upon the front lens. For the purpose of the ray tracing simulations, a single $2.9 \times 2.9 \text{ mm}^2$ square pixel of the PMT is approximated as a circle of diameter 3.3 mm, giving the equivalent circular area. Figure 3 shows the optical system layout and the point spread function (PSF). The PCE is shown in Figure 4, alongside the RMS spot size as a function of field angle. The results are achieved using a simulation

Table 1: Parameters of the Mini-EUSO instrument, including the field of view (FoV) for each independent pixel. Parameters for the proposed JEM-EUSO instrument are also shown (Adams et al., 2015a), along with the EUSO-SPB pathfinder and TUS for comparison (Wiencke, 2015, Adams et al., 2015b). Mini-EUSO is defined as a pathfinder for the JEM-EUSO mission and as such, the FoV and pixel size for Mini-EUSO were chosen to give a comparable UV signal and exposure. The spatial resolution given is the extent of a single pixel on the Earth’s surface for a nadir-pointing instrument. Pixel size on the MAPMT for all EUSO instruments is a circle of 3.3 mm diameter, whereas for TUS the pixel is a single circular PMT of diameter 13 mm.

	Mini-EUSO	JEM-EUSO	EUSO-SPB	TUS
Spatial resolution	5 km	560 m	130 m	5 km
Temporal resolution	2.5 μ s	2.5 μ s	2.5 μ s	800 ns
Aperture shape	Circular	Circular	Square	Hexagonal segments
Aperture area	490 cm ²	4.5×10^4 cm ²	1×10^4 cm ²	2×10^4 cm ²
FoV	44°	60°	11°	9°
FoV/Pixel	0.8°	0.08°	0.23°	0.8°
N° pixels	2304	315 648	2304	256

run with 3 wavelengths of 337 nm, 357 nm and 391 nm, each with equal intensity. This gives an approximation of the chromatic response over the accepted wavelength band of 300 - 400 nm, for the primary emission lines of EAS-induced air fluorescence (Kakimoto et al., 1996). Factors due to surface reflection, material absorption, surface roughness and Fresnel facet back cut are also taken into account. In addition to the optical system of Mini-EUSO, it is important to recall that Mini-EUSO will be positioned looking through a UV-transparent, nadir-facing window in the Russian Zvezda module. The transmission function

of this window is fairly constant at a value of 86% over a wide wavelength range, including the 300 - 400 nm band detected by Mini-EUSO. This is not included in the simulated instrument response as it will not affect the results, just slightly increase the thresholds.

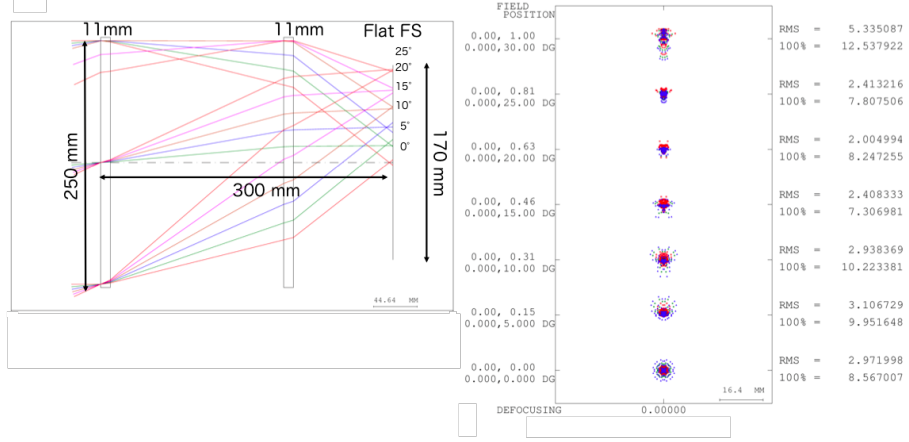


Figure 3: The left figure shows the lens design of Mini-EUSO configuration. Key dimensions are shown in bold text. The lenses are 11 mm thick, the focal length is 300 mm and the FS (focal surface) is a square of side 170 mm. In the figure on the right, the PSF is shown for a range of field positions. Incoming light is parallel with different inclinations as shown on the left of the figure. The RMS and 100% values are given in units of mm.

The array of MAPMTs in the Mini-EUSO PDM is powered by a Cockroft-Walton high voltage power supply (HVPS), allowing for a low power solution to providing the high voltage needed by the PMTs. In order to protect the MAPMTs from potentially damaging high current levels, the HVPS has a fast ($< 3 \mu\text{s}$) built-in switch which drastically reduces the gain of the MAPMTs when the anode current surpasses a threshold value. The photon flux of the phenomena which will be observed by Mini-EUSO varies on the order of 10^6 , from background levels of 1 count/pixel/GTU (1 GTU = $2.5 \mu\text{s}$), to bright TLEs and meteors. The background value stated is the number of photons detected by Mini-EUSO (photon counts). This value obtained for JEM-EUSO by Adams Jr et al. (2013), scales roughly in the same way to Mini-EUSO, taking into account

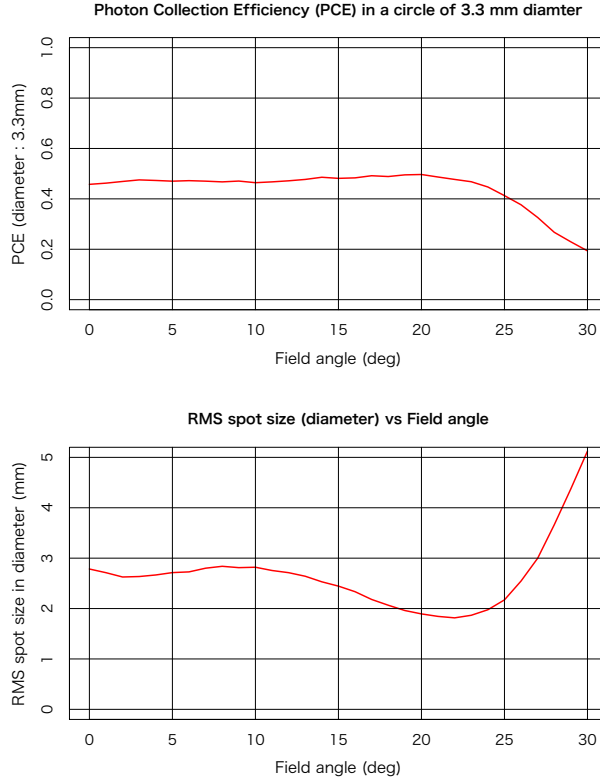


Figure 4: Top: The photon collection efficiency in 1 pixel (a circle of diameter 3.3 mm) as a function of the angle at which photons enter the first lens. Bottom: The RMS spot size in mm, also as a function of field angle.

the ratio of the optics size and pixel field of view. The HVPS handles this large range via the implementation of a second switch, controlled by the Zynq board. This second switch works by reducing the gain in a controlled way, as the incident photon flux increases in order to cover the full dynamic range of 10^6 , without damage to the MAPMTs. The anode current is continuously monitored and higher gain is restored once the current has dropped beneath the threshold level.

The data acquisition system consists of the front-end electronics, the PDM-DP (PDM data processing) sub-system based on a Xilinx Zynq XC7Z030 (Xil-

inx, 2016) system on chip and a PCIe/104 form factor CPU. This is an evolution of the system used in previous EUSO pathfinders, such as EUSO-TA, EUSO-Balloon and EUSO-SPB, incorporating the functionality of several subsystems into one board. Incoming photon pulses are pre-amplified and digitised by the SPACIROC3 ASICs (Blin-Bondil, S et al., 2014) at intervals of $2.5\text{ }\mu\text{s}$, referred to as the Gate Timing Unit or GTU. The signal is then triggered and time-stamped in the Zynq FPGA, before being passed to the CPU for data management and storage. The Zynq chip contains a Xilinx Kintex7 FPGA, with an embedded dual core ARM9 CPU processing system and is responsible for of the majority of the data handling including data buffering, configuration of the SPACIROC3 ASICs, triggering, synchronisation and interfacing with the separate CPU system. In addition, the high-voltage applied to the PMTs is also controlled here, allowing fast real-time response to high signal. The data acquisition system is summarised in Figure 5. The CPU performs the control of the instrument subsystems as well as the data management and storage, housekeeping, switching between operational modes and collecting data from the NIR and VIS cameras. Data is stored on board in SSDs which are periodically returned to Earth from the ISS, as it is not possible to telemeter such a large amount of data. In order to monitor the status of the Mini-EUSO instrument, smaller “quick-look” data samples will be telemetered at regular intervals by the astronauts on board the ISS. The instrument has no direct connection to the ISS network, so time-stamping will be achieved using the on-board CPU clock, which is regularly synchronised with the Zynq FPGA. In addition to this, Mini-EUSO will make observations of a ground-based laser system (as described in Section 3.1) which will allow offline synchronisation of the on-board CPU and use of the publicly available ISS ephemeris data in the subsequent analysis (NORAD Two-Line Element sets, The Center for Space Standards & Innovation (2017)).

A multi-level trigger system is implemented in the Zynq programmable logic in order to maximise the scientific output of the instrument. The motivation for this is to capture events of interest on short timescales whilst continuously imaging and mapping the UV emissions. EECR-like events are triggered with

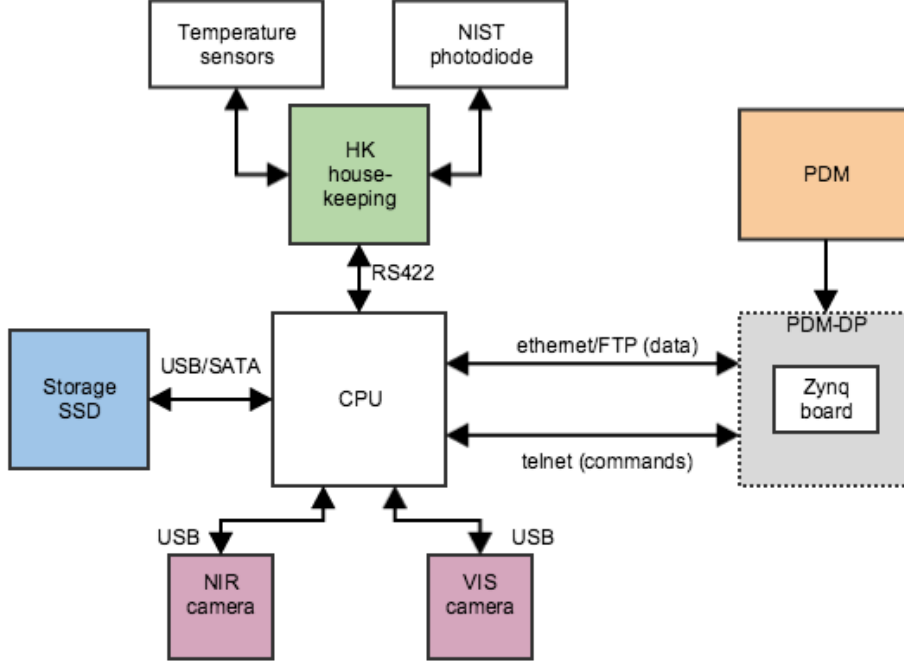


Figure 5: The data acquisition system of Mini-EUSO with the main interfaces shown. Incoming data from the PDM ASICs is triggered in the Zynq board and then passed to the CPU via an ethernet link. The CPU combines this data with that of the housekeeping system and the ancillary cameras. Data is then moved to onboard SSDs for storage.

a resolution of $2.5\ \mu\text{s}$ (L1 trigger), TLEs with a resolution of $320\ \mu\text{s}$ (L2 trigger) and there is an additional continuous readout with a resolution of $40.96\ \text{ms}$ (L3 data). For the L1 trigger logic, each pixel is considered as independent due to its large field of view at ground of $6.11\ \text{km}$, thus photons traveling at the speed of light take $\sim 20\ \mu\text{s}$ to cross one pixel. The background level is calculated over 128 GTU ($1\ \text{GTU} = 2.5\ \mu\text{s}$) and used to set a threshold of 8σ over the background level. The 128 GTU of integrated data used to calculate the background level is also passed as an input to the L2 trigger. Signal in a single pixel is integrated over 8 GTU and when the threshold is surpassed, the event is triggered and the whole 128 GTU packet is stored, centred on the event. The L2 trigger functions analogously but instead takes an integrated input of

1 GTU_{L2} = 320 μ s. The L2 also passes 128 integrated GTU_{L2} = 1 GTU_{L3} = 40.96 ms to the next level of the trigger algorithm. Key parameters of the trigger algorithm, such as the threshold and integration period, are configurable and can be changed in-flight. Every 5.24 s the three data types are read out to the CPU for permanent storage along with housekeeping data. A more detailed description of the trigger algorithm and the PDM-DP system is given in Belov et al., (submitted).

The NIR and VIS cameras will operate with a trigger passed from the Mini-EUSO PDM in order to provide multi-wavelength measurements of slower atmospheric events, such as meteors and nuclearites. When not triggered, the cameras will operate continuously to provide complementary measurements on the atmospheric status at the time of measurement, matching the third level of data from the Mini-EUSO trigger.

3. Mission objectives

3.1. Scientific objectives

The objective of Mini-EUSO is to perform, for the first time, high-resolution mapping of the emission from the night-Earth in the UV band (300 - 400 nm), in order to study the UV luminosity. Previous missions, for example the Tatiana experiment (Garipov et al., 2005), with a spatial resolution of ~ 100 km, have found a minimum flux level of the order of 3×10^{11} photons \cdot m⁻² s⁻¹ sr⁻¹. However, this is an estimate for the dark areas of the Earth during moonless nights, with values a factor of 2-5 higher being possible over clouds or cities and 1-2 orders of magnitude higher over aurora regions. Other balloon-borne experiments such as EUSO-Balloon and BABY (Catalano et al., 2002), have also made higher resolution (of the order of 10 km) measurements of the UV emission over ground, but only in localised areas and at altitudes below 40 km, meaning they are unable to detect airglow emission, aurora or other high-altitude effects. NIGHTGLOW has made measurements with a resolution of ~ 3 km from an altitude of 30 km at a range of zenith angles from nadir to

45° off-zenith, allowing observation of the airglow emission. The results, as presented in Barbier et al. (2005), show that airglow emission can contribute to an increase in the UV emission level of a factor of ~ 2.6 . Mini-EUSO will observe with a temporal resolution of 2.5 μ s and a spatial resolution of 6.11 km and as such will be able to characterise the UV luminosity of the entire Earth with unprecedented detail.

TLEs such as blue jets, sprites and elves have been discovered relatively recently and are still not well understood. A detailed review of developments in the experimental and modeling studies of TLEs is presented in Pasko et al. (2011). These upper-atmospheric events are luminous in the UV and have high frequencies (Garipov et al., 2010, Panasyuk et al., 2010), thus should be well characterised to avoid interference with EECR detection and triggering. Mini-EUSO has a dedicated trigger algorithm to capture TLEs and other millisecond scale phenomena at high resolution. This data could help improve the understanding of the formation mechanisms of these filamentary plasma structures, complementing atmospheric science experiments SMILES (Randel and Wu, 1996) and ASIM (Neubert and Team, 2009). Figure 6 shows examples of typical TLEs as Mini-EUSO is expected to detect them (see Table 3 for the definition of typical TLE parameters). The HV switching system of Mini-EUSO will modify the detection efficiency of the MAPMTs by changing the voltage between cathode and the first dynodes, as described in Section 2. In this way, the full dynamic range of Mini-EUSO spans over 6 orders of magnitude in photon flux and many different types of TLEs can be detected.

Mini-EUSO will also be able to see slower events such as meteors, fireballs, strange quark matter (SQM) and space debris with magnitudes of $M < +5$. In optimal dark conditions, the signal (integrated at steps of 40.96 ms) will exceed the UV-nightglow level by 3 - 4σ . These events will be detected using offline trigger algorithms on ground, although it is also possible that bright meteor events that appear suddenly can be triggered by the level 2 trigger, allowing higher resolution data for such events. Table 2 shows the expected rate of meteors and intensity of the signal as a function of the magnitude. Figure 7

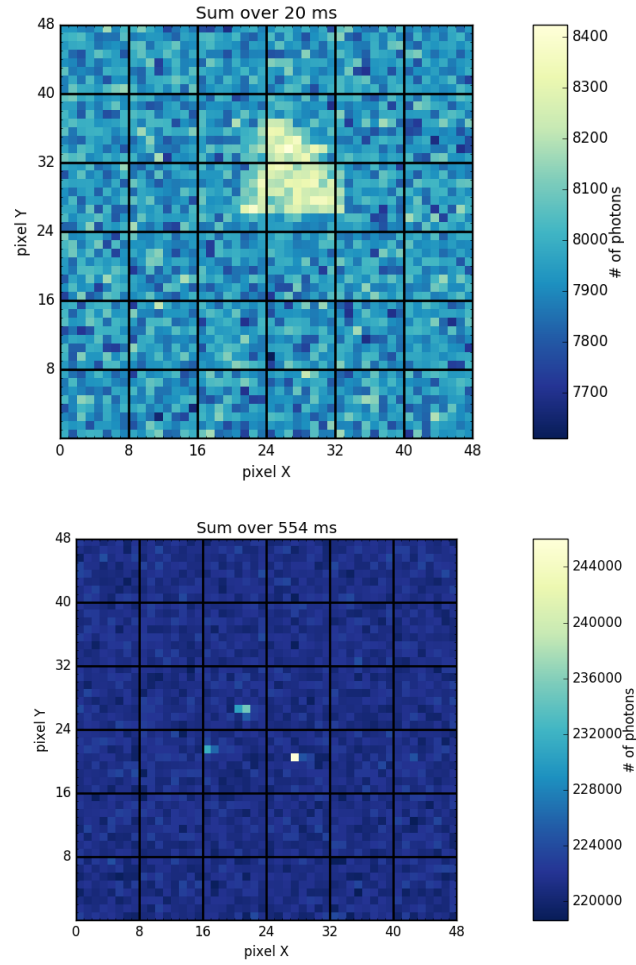


Figure 6: Expected light track of a diffuse elf (top) and 3 localised blue jet events (bottom) as they would be detected by Mini-EUSO. Background emission is also included, centred on 1 photon count/pixel/GTU (Adams Jr et al., 2013).

Table 2: Meteor emissions expected by Mini-EUSO. For a range of values of absolute magnitudes in visible light, the table lists the corresponding flux in the U -band of the Johnson-Morgan UBV photometric system (Spitzer Science Center, 2016), numbers of photons/second (assuming that the meteor is located at a height of 100 km and is observed by the ISS in the nadir direction) and photo-electrons/ms for Mini-EUSO. The typical mass of the meteor, and the number of events expected to be observed by Mini-EUSO (by assuming a duty cycle of 0.2) are also shown. The relationship between mass and magnitude has been obtained following Robertson and Ayers (1968). For more details see Abdellaoui et al. (2016).

Abs. mag	U-band flux (erg/s/cm²/Å)	photons (s⁻¹)	photo-e⁻ ms⁻¹	mass (g)	event rate
+5	$4.2 \cdot 10^{-11}$	$2.7 \cdot 10^8$	10^2	10^{-2}	2.4/min
0	$4.2 \cdot 10^{-9}$	$2.7 \cdot 10^{10}$	10^4	1	0.11/orbit
-5	$4.2 \cdot 10^{-7}$	$2.7 \cdot 10^{12}$	10^6	100	2.5/year

shows an example of a meteor track having absolute magnitude $M = +5$ crossing the field of view of Mini-EUSO with a 45° inclination with respect to the nadir axis. The meteor speed is 70 km s^{-1} and its duration is 2 s.

Even after just 1 month of observation at a minimal UV-nightglow level, Mini-EUSO will be able to set a new upper limit on the detection of SQM, as shown in Figure 8. SQM is composed of roughly equal numbers of up, down and strange quarks, and can form stable macroscopic nuggets referred to as nuclearites (De Rujula and Glashow, 1984). As described in Adams Jr et al. (2014a), these nuclearites create a UV signal upon interaction with the atmosphere which can be detected by Mini-EUSO. The nuclearite signal is easily discerned from meteor tracks as we expect much higher velocities on the order of $\sim 100 \text{ km s}^{-1}$, compared to a maximum of around 72 km s^{-1} for meteors. Figure 8 shows the upper limit on the nuclearite flux of $10^{-21} \text{ cm}^{-2} \text{ sr}^{-1} \text{ s}^{-1}$ for a null detection of nuclearites based on the conservative assumption that events with a projected velocity below 190 km s^{-1} are rejected.

The observation of space debris is also a highly relevant issue. Mini-EUSO is effectively a high-speed camera with a large field of view and will be used

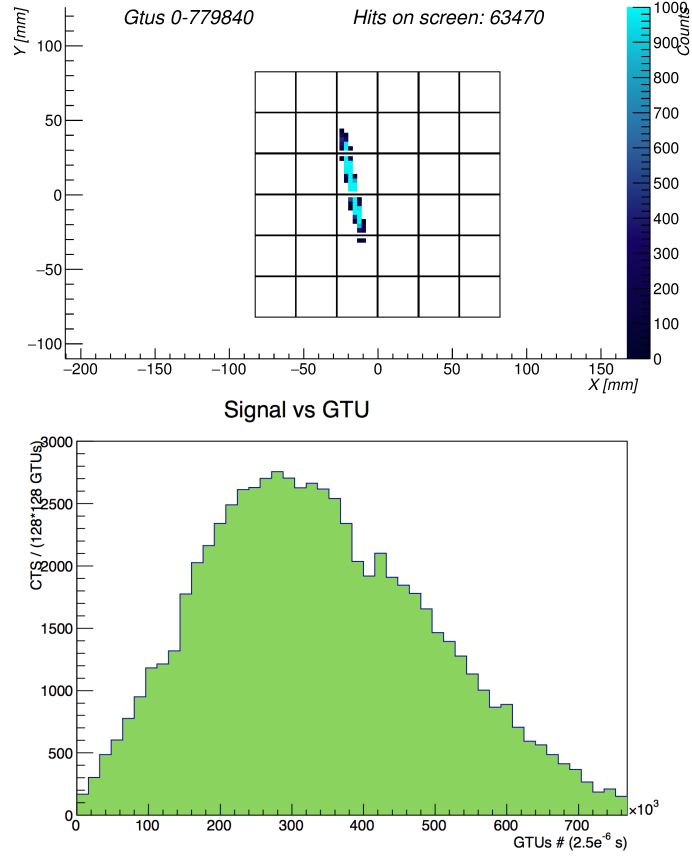


Figure 7: Top: Expected light track of a meteor of absolute magnitude $M = +5$ detected by Mini-EUSO (the effects of UV-nightglow are not included and a threshold has been applied at 30 counts). Bottom: Expected light profile. Each time bin on the x-axis corresponds to an integration time of 40.96 ms, the resolution of the level 3 data from Mini-EUSO. Figure taken from Abdellaoui et al. (2016).

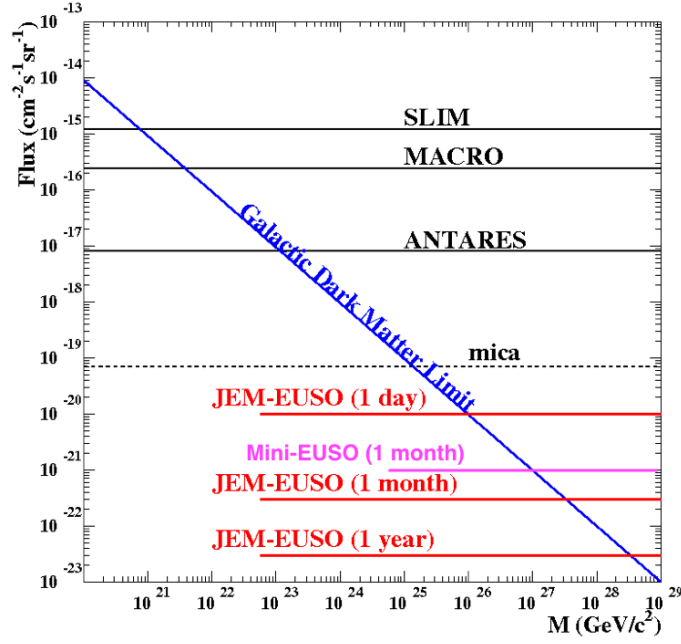


Figure 8: The 90% confidence level upper limit to SQM with Mini-EUSO after 1 month of observation as compared to the limits set by other experiments: MACRO (Ambrosio et al., 2000), SLIM (Sahnoun, 2009), ANTARES (Pāvālaš and the ANTARES Collaboration, 2013) and MICA (Price, 1988). The limits achieved by the planned JEM-EUSO instrument are also shown, these are stronger as JEM-EUSO has an aperture of around 4 times the size of Mini-EUSO, as well as a higher duty cycle and lower energy threshold.

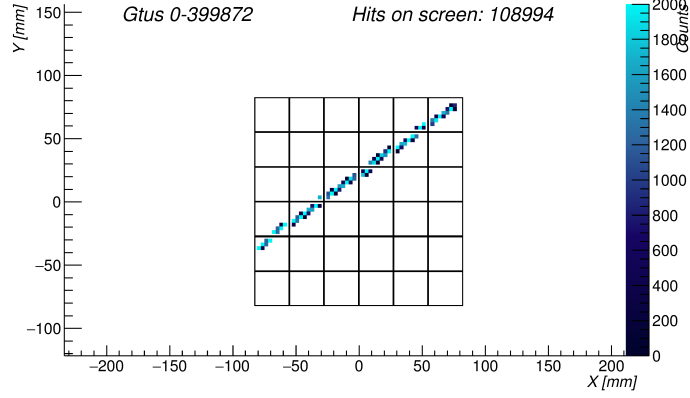


Figure 9: Expected light track of a piece of space debris flying at a relative speed of 10 km s^{-1} at an altitude of 10 km below the ISS whose signal is ~ 100 counts/ms on the Mini-EUSO focal surface. The track is followed for 1 s (the effects of UV-nightglow are not included and a threshold has been applied at 30 counts).

as a prototype for the detection of space debris during the twilight periods of observation (when debris are illuminated by the sun, but the instrument is in darkness). In the future, larger scale EUSO experiments could be used in conjunction with a novel high efficiency fibre-based laser system (CAN) to provide a space-based debris remediation system (Ebisuzaki et al., 2015). Figure 9 shows an example of integrated track of a space debris flying at a speed of 10 km s^{-1} at an altitude of 10 km below the ISS. The signal is 100 counts/ms on the Mini-EUSO focal surface and the track is followed for 1 s, during which the signal is assumed to be constant and no UV-nightglow light has been added. This is preliminary work that shows the potential of Mini-EUSO for debris detection, a more realistic implementation of the expected signal in Mini-EUSO as a function of the size of the debris, as well as its reflectance and illumination by the sun, is currently under development.

Although Mini-EUSO is not designed to detect EECRs due to the small size of the optical system, it is still possible to detect cosmic rays above the energy threshold of $E_{thr} \sim 1 \times 10^{21} \text{ eV}$ (see Figure 10). Existing results from both ground-based facilities Telescope Array and the Pierre Auger Observatory

show that we should not expect to detect EECRs at such high energies due to the observation of the GZK suppression at $(5.4 \pm 0.6) \times 10^{19}$ eV and $(2.9 \pm 0.2) \times 10^{19}$ eV respectively (Abu-Zayyad et al., 2013, Abraham et al., 2010). In this way, Mini-EUSO will likely provide an upper limit for a null detection with its large annual exposure of $\sim 15\,000\text{ km}^2\text{ sr}$. This value of the exposure assumes an observational duty cycle of 20%, as well as effects due to clouds and localised light sources in the FoV. The calculation follows the method presented for JEM-EUSO in Adams Jr et al. (2013). Figure 11 shows the expected track (top) and light curve (bottom) of a EECR with energy $E = 1 \times 10^{21}$ eV and inclination of 80° to the nadir that would be triggered by the first level trigger of Mini-EUSO in standard UV nightglow illumination of ~ 1 photon count/pixel/GTU (Adams Jr et al., 2013). As shown in Figure 10, such an event is triggered with an efficiency of $\sim 40\%$, and thus is on the threshold of detection. Background is not included in the figure in order to show the structure of the EECR signal, but is implemented in the simulation chain to properly test the trigger logic.

Additionally, during flight it will be possible to simulate EECR-like signals using ground-based laser facilities in order to verify the capability of Mini-EUSO to detect cosmic rays and to allow the testing and optimisation of the trigger system. The GLS (Global Light System) has been developed for the JEM-EUSO project in order to provide a means of in-flight calibration via benchmark optical signatures with known rate, intrinsic luminosity, time and direction (Adams Jr et al., 2014b). The GLS laser prototype is currently in operation: a portable, steerable, 90 mJ and 355 nm laser system based at the Colorado School of Mines. It has been successfully tested both during the flight of EUSO-Balloon (Eser, 2016) and more recently in the calibration of the EUSO-TA and EUSO-SPB instruments. Even with one fixed, ground-based station, a laser campaign during the ISS overpass is feasible, with an opportunity around once every 2 months during the flight of Mini-EUSO. Simulations show that a 80 mJ, unpolarised laser, fired perpendicular to the ISS motion with an elevation angle of 25° would produce a signal comparable in both intensity and duration to an EAS produced

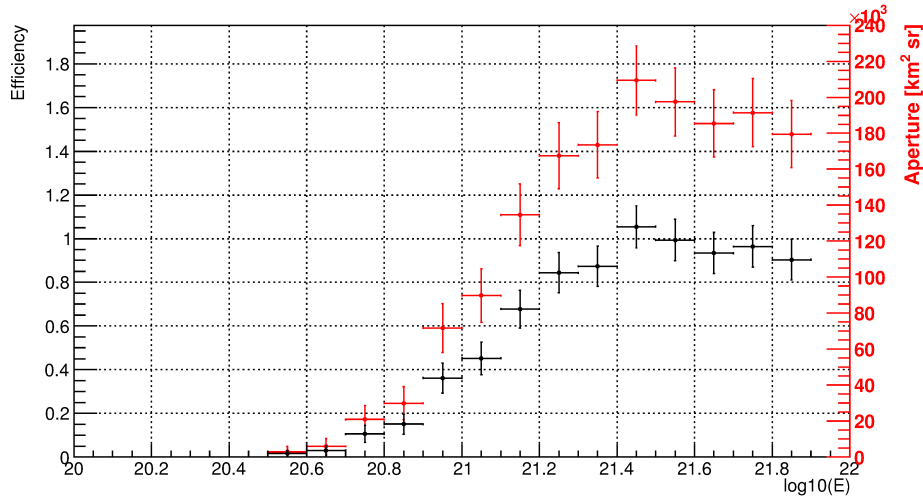


Figure 10: The detection efficiency (on the left axis, in black) and geometry factor, i.e. geometry factor, (on the right axis, in red) are shown as a function of the EAS energy, E , in eV. A UV background level of 1 photon count/pixel/GTU (Adams Jr et al., 2013) was considered in both cases.

by an EECR of $\sim 10^{21}$ eV (see Figure 11).

Other scientific objectives of Mini-EUSO include observation of the bioluminescence of the sea from space. Since 1915, there have been 255 documented reports of *milky sea* (Great Britain Meteorological Office Marine Division, 1993) and even more events have been reported historically. The *milky sea* or *mareel* is a term used to describe conditions where large areas of the ocean surface (up to $16,000 \text{ km}^2$) appear to glow during the night for periods of up to several days. The condition is poorly understood, but typically attributed to the bioluminescence of the luminous bacteria *Vibrio harveyi* in connection with the presence of colonies of the phytoplankton *Phaeocystis*. The bioluminescent bacteria have been shown in the laboratory to have an emission spectra which peaks at 490 nm with a bandwidth of 140 nm (Hastings and Morin, 1991, Seliger and Morton, 1968). There has been a single report of satellite observations of this phenomenon, confirmed by a ship-based account (Miller et al., 2005). Whilst the BG3 filter on the Mini-EUSO MAPMTs is optimised for the 300 - 400 nm

band, it extends up to 500 nm and Mini-EUSO is able to detect $\sim 20\%$ of the bioluminescence spectrum. Taking this into account, for a signal of 5σ above the background level of 1 photon count/pixel/GTU (Adams Jr et al., 2013) in a single pixel of Mini-EUSO, the limiting source radiance of the bacteria is $\sim 10^{10}$ photons/cm²/s. This number should be regarded as approximate as the true sensitivity also depends on the spatial extent of the signal on the focal plane and the background level, which is dependent of the atmospheric conditions at the time of observation. 5σ in a single pixel is stringent requirement for a signal that is expected to cover a significant portion of the focal surface for a duration of around 20 s. The response of Mini-EUSO is included, and atmospheric attenuation has been neglected. This estimate gives an order of magnitude higher sensitivity than the value of 1.4×10^{11} photons/cm²/s reported in Miller et al. (2005), following a successful detection. Further detections of the milky sea events from space could deeply enhance the understanding of this elusive phenomena, as well as the distribution and transport of phytoplankton on a global scale.

3.2. Technological objectives

In addition to the scientific objectives, Mini-EUSO will address important technology issues regarding the future of EECR detection from space. Mini-EUSO will be the first use of a Fresnel-based optics system in space and will provide the opportunity to validate the JEM-EUSO observation scheme on the scale of one module. The technology readiness level of the JEM-EUSO instrumentation will also be raised by this mission providing important spaceflight qualification and heritage of the hardware.

4. Simulations of typical observations

The Mini-EUSO configuration has been included in the ESAF (EUSO Simulation and Analysis Software) package. ESAF is the official software tool to perform simulations of EAS development, photon production and transport

through the atmosphere and detector response for optics and electronics. Moreover, ESAF includes algorithms for the reconstruction of the properties of air showers produced by EECRs. Originally developed for the ESA-EUSO mission, all the planned missions of the JEM-EUSO program have been implemented in ESAF in order to assess the full range of expected performances for cosmic ray observation (Bertaina et al., 2014). The simulation and modeling of EECR events in ESAF is detailed in Berat et al. (2010). All simulated data shown in Section 3.1 has been generated using ESAF.

Table 3: Typical key parameters used in the modelling of TLEs implemented in ESAF. The altitude, radius and extension all refer to the maximum values reached in the development of the simulation. For blue jets, the angle of the jet with respect to the vertical can also be defined and a typical value is 15° . Faint TLEs are simulated here in order to test the sensitivity of Mini-EUSO to such events.

	Altitude	Abs	Radius	Extension	Duration
	[km]	mag.	[km]	[km]	[ms]
Blue Jets	60	2	0.3	4	15
Sprites	80	1	1	2	10
Elves	80	1	50	1	20

Recently the simulation of slower events, such as TLEs, meteors and space debris has also been implemented in the ESAF framework. It is possible to simulate 3 different types of TLE: blue jets, sprites and elves. Blue jets are modelled as an expanding cone of light in the atmosphere with the emission spectra dominated by the second positive N_2 and the first negative N_2^+ bands as detailed in Pasko and George (2002). Sprites are modelled as an expanding light cone with a hemispherical top, and are defined similarly to blue jets. Elves are modelled as larger expanding disks of light with a central hole and a spectral profile as described in Chang et al. (2010). In each case, key parameters define the size and shape, duration, development and brightness of the TLEs. Typical values for these parameters are shown in Table 3. Meteors are modelled using

a simple simulator which allows the specification of the initial meteor altitude, the velocity vector, the event duration and the morphology of the light curve due to meteoroid ablation. The possibility of simulating flares in the emission of the meteor during its passage through the atmosphere is also implemented, with flare start time, duration and light curve morphology being further input parameters. More details of the approach to meteor simulation can be found in Abdellaoui et al. (2016). The modelling of space debris is currently under development. Debris are modelled as spherical and implemented in a similar manner to that of meteors, but taking into account the geometry of the illumination and the kinematics in the field of view.

5. Conclusion

In summary, Mini-EUSO is a compact UV telescope that will be placed at a nadir-facing window inside the Zvezda module of the ISS. The instrument employs a multi-level trigger system. This allows it to capture interesting events on the time scales of EECR-induced atmospheric showers and TLEs with a high temporal resolution, whilst also providing a continuous readout with a resolution of 40.96 ms. Mini-EUSO will provide insight into a variety of atmospheric and terrestrial UV phenomena (with complementary information from the NIR and visible light cameras) as well as raising the technology readiness level of future EUSO missions. Typical observations have been simulated in order to verify the mission goals and to test the trigger algorithm. Mini-EUSO is approved as a joint project by the Italian (ASI) and Russian (Roscosmos) space agencies and the instrument integration is currently at an advanced stage to be on schedule with a possible launch in late 2017 to early 2018.

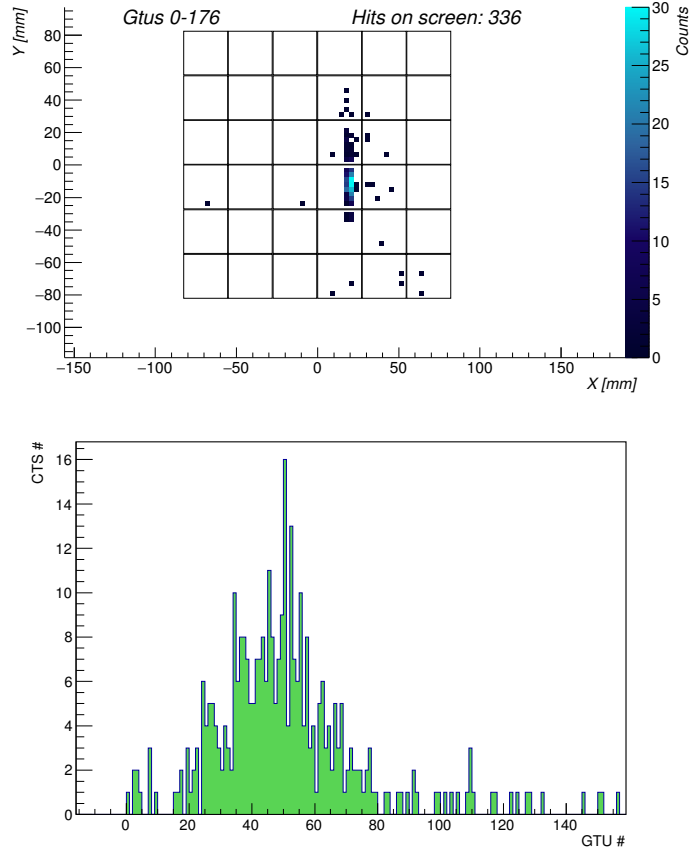


Figure 11: Top: Photon counts observed in the Mini-EUSO focal surface for a simulation of an $E = 1 \times 10^{21}$ eV event with an inclination of 80° to the nadir. Bottom: Light curve for the same event. The x-axis shows time in units of GTU (1 GTU = $2.5 \mu\text{s}$). Background of 1 photon count/pixel/GTU is not included in the simulation, in order to clearly show the track structure. Whilst it is not expected that Mini-EUSO will detect an event of such high energy, this event gives a fair representation of the signal that is expected to be seen by Mini-EUSO when the ground-based laser system is used to test the trigger logic, thus verifying the EUSO detection principle.

Acknowledgements

This work was partially supported by the Italian Ministry of Foreign Affairs and International Cooperation, Italian Space Agency (ASI) contract 2016-1-U.0, the Russian Foundation for Basic Research, grants #15-35-21038 and #16-29-13065, and the Olle Engkvist Byggmästare Foundation. We acknowledge useful discussions with M. Bertaina and F. Fenu regarding the ESAF simulations and also the contribution of Y. Takizawa in the simulation of the Mini-EUSO optical system. The anonymous referees are also thanked for their detailed and constructive input. The authors would like to dedicate this paper to the memory of Dr. Jacek Karczmarczyk and Dr. Yoshiya Kawasaki, who have contributed greatly to the collaboration and will be deeply missed.

References

References

- G. Abdellaoui, S. Abe, A. Acheli, et al. Meteor studies in the framework of the JEM-EUSO program. *Planetary and Space Science*, 143:245–255, 2016.
- J. Abraham, P. Abreu, M. Aglietta, et al. Measurement of the energy spectrum of cosmic rays above 10^{18} eV using the Pierre Auger Observatory. *Physics Letters B*, 685(4-5):239–246, Mar. 2010.
- T. Abu-Zayyad, R. Aida, M. Allen, R. Anderson, et al. The cosmic-ray energy spectrum observed with the surface detector of the Telescope Array experiment. *The Astrophysical Journal Letters*, 768(1):L1, May 2013.
- J. H. Adams, S. Ahmad, J. N. Albert, et al. The JEM-EUSO instrument. *Experimental Astronomy*, 40(1):19–44, 2015a.
- J. H. Adams, S. Ahmad, J. N. Albert, et al. Space experiment TUS on board the Lomonosov satellite as pathfinder of JEM-EUSO. *Experimental Astronomy*, 40(1):315–326, Nov. 2015b.

- J. H. Adams Jr, S. Ahmad, J. N. Albert, et al. An evaluation of the exposure in nadir observation of the JEM-EUSO mission. *Astroparticle Physics*, 44: 76–90, Apr. 2013.
- J. H. Adams Jr, S. Ahmad, J. N. Albert, et al. JEM-EUSO: Meteor and nuclearite observations. *Experimental Astronomy*, 40(1):253–279, 2014a.
- J. H. Adams Jr, M. J. Christl, S. E. Csorna, et al. Calibration for extensive air showers observed during the JEM-EUSO mission. *Advances in Space Research*, 53(10):1506–1514, May 2014b.
- M. Ambrosio, R. Antolini, C. Aramo, et al. Nuclearite search with the MACRO detector at Gran Sasso. *Eur. Phys. J. C*, 13(hep-ex/9904031. 3):453–458, 2000.
- L. M. Barbier, R. Smith, S. Murphy, et al. NIGHTGLOW: an instrument to measure the Earth’s nighttime ultraviolet glow—results from the first engineering flight. *Astroparticle Physics*, 22(5-6):439–449, Jan. 2005.
- A. Belov, F. Capel, F. Fausti, et al. The integration and testing of the Mini-EUSO multi-level trigger system. *Advances in Space Research*. (submitted).
- C. Berat, S. Bottai, D. De Marco, S. Moreggia, et al. Full simulation of space-based extensive air showers detectors with ESAF. *Astroparticle Physics*, 33(4):221–247, May 2010.
- M. Bertaina, S. Biktmerova, K. Bittermann, et al. Performance and air-shower reconstruction techniques for the JEM-EUSO mission. *Advances in Space Research*, 53(10):1515–1535, May 2014.
- Blin-Bondil, S, Barrillon, P, and Dagoret-Campagne, S. SPACIROC3: A Front-End Readout ASIC for JEM-EUSO cosmic ray observatory. In *Proceedings of the 3rd International Conference on Technology and Instrumentation in Particle Physics (TIPP)*, Amsterdam, page PoS(TIPP2014)172, 2014.

- O. Catalano, G. Agnetta, B. Biondo, et al. The atmospheric nightglow in the 300 – 400 nm wavelength Results by the balloon-borne experiment BABY. *Nuclear Instruments and Methods in Physics Research Section A*, 480(2-3): 547–554, Mar. 2002.
- S. C. Chang, C. L. Kuo, L. J. Lee, et al. ISUAL far-ultraviolet events, elves, and lightning current. *Journal of Geophysical Research: Space Physics*, 115 (A7):A00E46, 2010.
- A. De Rujula and S. L. Glashow. Nuclearites: A Novel Form of Cosmic Radiation. *Nature*, 312(5996):734–737, 1984.
- T. Ebisuzaki, M. N. Quinn, S. Wada, et al. Demonstration designs for the remediation of space debris from the International Space Station. *Acta Astronautica*, 112:102–113, 2015.
- J. Eser. EUSO-Balloon: Observation and Measurement of Tracks from a Laser in a Helicopter. *PoS*, ICRC2015:638, 2016.
- FLIR Integrated Imaging Solutions. Firefly MV USB 2.0 or 1394A, 2017a. URL <https://www.ptgrey.com/firefly-mv-13-mp-color-usb-2-sony-imx035?useripforwarding=false>.
- FLIR Integrated Imaging Solutions. Chameleon P/N: CMLN-13Y3C, USB 2.0, 2017b. URL <https://www.ptgrey.com/chameleon-13-mp-mono-usb-2-sony-icx445-camera?useripforwarding=false>.
- G. K. Garipov, B. A. Khrenov, M. I. Panasyuk, et al. UV radiation from the atmosphere: Results of the MSU “Tatiana” satellite measurements. *Astroparticle Physics*, 24(4-5):400–408, Dec. 2005.
- G. K. Garipov, B. A. Khrenov, P. A. Klimov, et al. Program of transient UV event research at Tatiana-2 satellite. *Journal of Geophysical Research: Space Physics*, 115(A5), 2010. ISSN 2156-2202. A00E24.

- Great Britain Meteorological Office Marine Division. *The Marine Observer*. Meteorological Office, London, 1993.
- J. W. Hastings and J. G. Morin. *Neural and integrative animal physiology*. Wiley-Liss: New York, 1991.
- F. Kakimoto, E. C. Loh, M. Nagano, et al. A measurement of the air fluorescence yield. *Nuclear Instruments and Methods in Physics Research Section A: Accelerators, Spectrometers, Detectors and Associated Equipment*, 372(3): 527–533, Apr. 1996.
- Y. Kawasaki, L. W. Piotrowski, and for the JEM-EUSO Collaboration. Ground-based tests of JEM-EUSO components at the Telescope Array site, “EUSO-TA”. *Experimental Astronomy*, 40(1):301–314, 2015.
- S. D. Miller, S. H. D. Haddock, C. D. Elvidge, and T. F. Lee. Detection of a bioluminescent milky sea from space. *Proceedings of the National Academy of Sciences*, 102(40):14181–14184, Oct. 2005.
- T. Neubert and A. I. Team. ASIM - an Instrument Suite for the International Space Station. In *Coupling of Thunderstorms and Lightning Discharge to Near-Earth Space: Proceedings of the Workshop*, volume 1118, pages 8–12, New York, 2009. AIP Publishing.
- A. V. Olinto, E. Parizot, M. Bertaina, and G. Medina-Tanco. JEM-EUSO Science. In *Proceedings of the 34th International Cosmic Ray Conference*, page PoS(ICRC2015)623, 2015.
- M. I. Panasyuk, V. V. Bogomolov, G. K. Garipov, et al. Transient luminous event phenomena and energetic particles impacting the upper atmosphere: Russian space experiment programs. *Journal of Geophysical Research: Space Physics (1978–2012)*, 115(A6):A00E33, 2010.
- V. P. Pasko and J. J. George. Three-dimensional modeling of blue jets and blue starters. *Journal of Geophysical Research: Space Physics*, 107(A12):SIA 12–1–SIA 12–16, Dec. 2002.

- V. P. Pasko, Y. Yair, and C.-L. Kuo. Lightning Related Transient Luminous Events at High Altitude in the Earth's Atmosphere: Phenomenology, Mechanisms and Effects. *Space Science Reviews*, 168(1-4):475–516, Sept. 2011.
- G. E. Păvălaș and the ANTARES Collaboration. Search for massive exotic particles with the ANTARES neutrino telescope. *Journal of Physics: Conference Series*, 409(1):012135, Feb. 2013.
- P. B. Price. Limits on Contribution of Cosmic Nuclearites to Galactic Dark Matter. *Phys. Rev.*, D38(12):3813–3814, 1988.
- W. J. Randel and F. Wu. Isolation of the ozone QBO in SAGE II data by singular-value decomposition. *Journal of the atmospheric sciences*, 53(17):2546–2559, 1996.
- J. B. Robertson and W. G. Ayers. NASA Technical Note D-4312;, 1968. URL <http://ntrs.nasa.gov/archive/nasa/casi.ntrs.nasa.gov/19680007281.pdf>.
- Z. Sahnoun. Search for strange quark matter and Q-balls with the SLIM experiment. *Radiation Measurements*, 44(9-10):894–897, Oct. 2009.
- V. Scotti and G. Osteria. EUSO-Balloon: The first flight. *Nucl. Instrum. Meth.*, A824:655–657, 2016.
- H. Seliger and R. Morton. A Physical Approach to Bioluminescence. *Photophysiology (Edited by AC Geise)*. Vol. IV, pages 253–314, 1968.
- Spitzer Science Center. Flux Density Converter , 2016. URL <http://ssc.spitzer.caltech.edu/warmmission/propkit/pet/magtojoy/index.html>.
- The Center for Space Standards & Innovation. NORAD Two-Line Element Sets, 2017. URL <https://www.celestrak.com/NORAD/elements/>.
- L. Wiencke. EUSO-Balloon mission to record extensive air showers from near space. In *Proceedings of the 34th International Cosmic Ray Conference*, page PoS(ICRC2015)631, 2015.

Xilinx. Zynq-7000 All Programmable SoC , 2016. URL <https://www.xilinx.com/products/silicon-devices/soc/zynq-7000.html>.